Reexamining the relationship of La Niña and the East Asian Winter Monsoon

Peng Zhang, Zhiwei Wu & Jianping Li

Climate Dynamics
Observational, Theoretical and Computational Research on the Climate System

ISSN 0930-7575
Volume 53
Combined 1-2

Clim Dyn (2019) 53:779-791
DOI 10.1007/s00382-019-04613-7

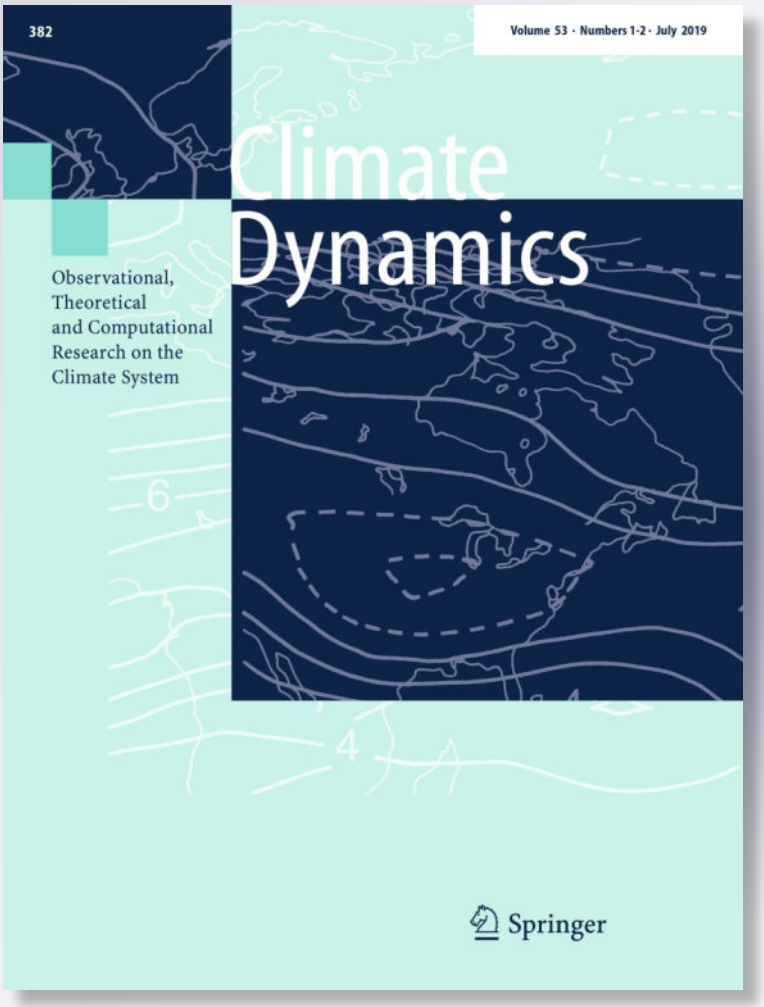

Springer

Climate Dynamics (2019) 53:779–791
https://doi.org/10.1007/s00382-019-04613-7

Reexamining the relationship of La Niña and the East Asian Winter Monsoon

Peng Zhang[1,2] · Zhiwei Wu[1] · Jianping Li[3]

Received: 17 June 2018 / Accepted: 3 January 2019 / Published online: 22 January 2019

Abstract
The northern and the southern modes are two distinct principle modes that dominate the winter mean surface air temperature (Ts) variations over East Asia (EA). The cold southern mode is represented by a significant cooling south of 45°N and is linked to La Niña events. An objective criterion, which could distinguish the spatial distributions and the maximum center of sea surface temperature anomaly (SSTA), is used to classify the La Niña events into two categories: mega-La Niña and equatorial La Niña. Their impacts are inspected onto the Ts southern mode. The mega-La Niña, featured by a significant K-shape warming in the western Pacific with the maximum SSTA cooling centered in the tropical central Pacific. As a response, an anomalous barotropic high is generated over North Pacific (NP) implying a weak zonal gradient between ocean and the EA continent, which induces a neutral Ts southern mode. The equatorial La Niña characterizes a significant cooling in the tropical eastern Pacific with convective descending motions shifting eastward to the east of the dateline. The resultant low-level circulation anomalies show an anomalous subtropical NP low and a gigantic abnormal EA continent high. The strong zonal gradient results in significant northerly anomalies over EA from 55°N to southeastern China. Over the mid-upper troposphere, the anomalous subtropical NP low extends westward to the Korean Peninsula, leading to a strengthened and southward shifted EA trough. Such abnormal circulation patterns favor the intrusion of cold air to southern EA and correspond to a strong Ts southern mode. The numerical results well validate the above processes and physical mechanisms.

1 Introduction

East Asian winter monsoon (EAWM) is a very active climate system in boreal winter, the members of which mainly include the Siberian high, mid-level trough, surface northerly and upper-level East Asian jet stream (Jhun and Lee 2004; Wang et al. 2010a; Wang and He 2012). This three-dimensional planetary-scale circulation features a baroclinic structure over East Asia (EA) (Ha et al. 2012). The variabilities of EAWM range from interannual to interdecadal timescale, which have been attributed to the influences of the Arctic Oscillation (Gong et al. 2001; Wu and Wang 2002) or the North Atlantic Oscillation (Wu and Huang 1999; Luo et al. 2016), the Atlantic Multi-decadal Oscillation (He and Wang 2013), the Eurasian pattern (Liu et al. 2014a, b; Wang et al. 2018), the blocking activities over Ural Mountain region (Wang et al. 2010a; Wang and Lu 2017) and the Southern Hemisphere annular mode (Wu et al. 2009). The El Niño and Southern Oscillation (ENSO)—as the most prominent interannual signal of air-sea interaction—could also profoundly impact on the EAWM (Tomita and Yasunari 1996; Zhang et al. 1996; Wang et al. 2000; Wang and Zhang 2002).

Many studies have proved that El Niño usually accompanies weak EAWM (Tao and Zhang 1998; Wang et al. 2000; Chen et al. 2000; Chen 2002; Zhang et al. 2015a, b), the situations are generally reversed during La Niña years (Wang et al. 2008). However, the degree of El Niño and La Niña events impact on the EAWM is asymmetric. For instance, Zhang et al. (1996) revealed that the El Niño appreciably weaken the EAWM, while La Niña does not significantly

✉ Zhiwei Wu
zhiweiwu@fudan.edu.cn

[1] Department of Atmospheric and Oceanic Sciences and Institute of Atmospheric Sciences, Fudan University, 2005 Songhu RD, Yangpu, Shanghai 200438, China

[2] State Key Laboratory of Numerical Modeling for Atmospheric Sciences and Geophysical Fluid Dynamics, Institute of Atmospheric Physics, Chinese Academy of Sciences, Beijing 100029, China

[3] Laboratory for Regional Oceanography and Numerical Modeling, Qingdao National Laboratory for Marine Science and Technology, Qingdao 266237, China

enhance it. Chen (2002) demonstrated that during El Niño winter, significant southerlies could be detected over the lower troposphere, but the northerlies are not that significant during La Niña winter. Still unclear, until now, is whether the influence of La Niña on EAWM is always weak or not.

Then, Wang et al. (2010a) revealed that there are two different principal modes—the northern mode (EOF1) and the southern mode (EOF2)—dominate the variabilities of winter mean surface air temperature (SAT) over the EA. For the southern mode, its positive phase shows a cooler than normal conditions over the whole subtropical EA, indicating a strong EAWM. They also pointed out that on the interannual time scale, the cold southern mode is associated with La Niña events. However, the atmospheric anomalies related to the cold SAT southern mode do not resemble that of conventional La Niña. Contrasting Fig. 1a (shown in Wang et al. 2010b, Fig. 6c) and 1b, huge differences are displayed over the North Pacific (NP). When a southern mode EAWM occur, over the surface level, an anomalous low is centered around 40°N and 190°W, accompanied by a salient anomalous EA continent high (Fig. 1a). The strong zonal gradient of the sea level pressure (SLP) anomalies between the NP and EA continent indicates strong northerly anomalies over EA, resulting in a strong EAWM (Wang et al. 2010b; Chen et al. 2014). During conventional La Niña winter (Fig. 1b),

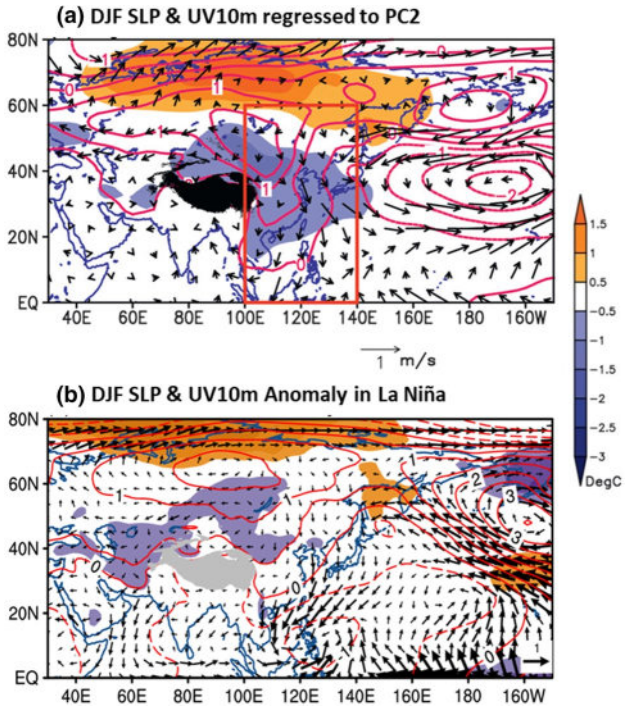

Fig. 1 **a** Sea level pressure (SLP, contours, hPa), Surface temperature (Ts, color shadings, °C), and surface winds (vectors, m/s) for anomalies regressed with reference to southern mode (Fig. 6c in Wang et al. 2010b). **b** SLP, 2 m temperature (T2m) (color shadings, K), and 10 m winds (UV10m) anomalies in La Niña

the strong anomalous high situated to the east of the Aleutian Islands with an anomalous low is centered over the Philippines. The weak land-sea SLP gradient implies weak northerlies over EA, leading to a neutral winter in the southern EA. So far, it seems that conventional La Niña cannot impact EAWM strongly. Therefore, is there a type of La Niña that can trigger the SLP anomalies over the NP region resembling SAT southern mode?

Recently, Jia et al. (2016) displayed that the negative SSTAs associated with cold SAT southern mode are concentered in the equatorial eastern Pacific (EP). The positive SSTAs in the western and subtropical NP, however, are not that significant compared with the conventional La Niña (see their Fig. 4h). This SSTA distribution highly resembles the Atypical ENSO pattern given by Zhang et al. (2016), who classified the ENSO events during their developing phase into two groups—the Typical and Atypical ENSO—using the mega-ENSO index. The latter type shows a spatial pattern that without significant tropical western and subtropical Pacific SSTA. Defined by Wang et al. (2013), the mega-ENSO index was calculated as the difference of averaged West Pacific K-shape SST and East Pacific triangle SST. It shows a spatial pattern that is similar to the Inter-decadal Pacific Oscillation (Power et al. 1999; Parker et al. 2007) or other decadal timescales ENSO-like variability (Zhang et al. 1997). Thus, comparing with traditional ENSO indices, it reflects a broader range of variability. As a new index, mega-ENSO has attracted much attention (Wu and Zhang 2015; Zhang et al. 2016, 2017). Therefore, whether the wintertime La Niña events can be divided by mega-ENSO and Niño3.4 indices?

This study aims to figure out what type of La Niña can significantly impact the EAWM. The text is structured as follows: data, model, experiment designs are presented in Sect. 2. Section 3 defines the two types of La Niña and shows their connections to the EAWM. Section 4 contrasts the dynamic structures of the different category of La Niña. The mechanisms through which La Niñas impact the EAWM are discussed in the Sect. 5. Section 6 gives a summary of the major findings.

2 Dataset, model and experiment design

In this study, the datasets cover from December 1957 to February 2017. Including: (1) monthly SST data from the merged (arithmetic mean) Extended Reconstructed Sea Surface Temperature (ERSST V4; Huang et al. 2014, 2015; Liu et al. 2014a, b) and Hadley Centre Global Sea Ice and Sea Surface Temperature (HadISST; Rayner et al. 2003) at 2°×2° horizontal resolution; (2) ERA-40 (Uppala et al. 2005) data for the period of September 1957 to December 1979, and ERA-interim (Dee et al. 2011) from January 1980

to February 2017 with horizontal resolution of 1.5° × 1.5°. The climatological difference between two datasets for the period of 1980–2002 is removed from 1980 to 2017 ERA-interim data to maintain temporal homogeneity; (3) the Niño3.4 index is calculated following the definition given by Climate Prediction Center (CPC); (4) the mega-ENSO index is defined as the difference between western Pacific K-shape SST and eastern Pacific triangle SST (Wang et al. 2013). One of the important features for mega-ENSO is to represent the gradient between eastern and western Pacific, which cannot be achieved by using Niño3.4, Niño3 or Niño4 indices. Winter refers to December–January–February (DJF) in this study. The deviation from the 60-year climatological mean (1957–2016) was conducted as anomalies for all variables. Considering the surface temperature data may contain an upward trend, we detrended the data from 1957 to 2016 to eliminate the long-term trend influence. We also used JRA-55 dataset for the analysis, the results were not changed (not shown).

The composite analysis was used in this paper. First, we normalized two indices to measure them at the same level. Both Niño3.4 and mega-ENSO indices (Fig. 2) show small linear trends—− 0.007 and 0.0072 respectively—not exceeding the Mann–Kendall trend significance test at 90% confidence level (Hamed and Rao 1998; Mondal et al. 2012). Figure 2b, c display the spectrum of Nino3.4 and mega-ENSO indices. The Nino3.4 index exhibits interannual time scale of variability, the peak is centered around 5 years. However, the spectral peak of the mega-ENSO index (around 11 years) is dominated by decadal timescales. The results suggest that the two indices not only represent a diverse spatial pattern, their time variations are also different. Then, based on the two time-series, we determined two types of La Niña events. If the normalized Niño3.4 index was less than − 0.5 and the mega-ENSO index was greater than 0.8, indicating the SSTAs pattern resembles that of mega-ENSO. The year met this criterion was determined as being a mega-La Niña event. Else, we selected the specific years as being the Equatorial (Eq.) La Niña event—if the normalized Niño3.4 index was less than − 0.5 and mega-ENSO index was less than 0.8, making sure that the significant SSTAs is confined to the equatorial region. 0.7 or 0.9 can also be chosen to divide the two types of La Niña event, which does not change the qualitative results.

The 5th generation Max-Plank-Institute Atmospheric General Circulation Model (AGCM), ECHAM5.4

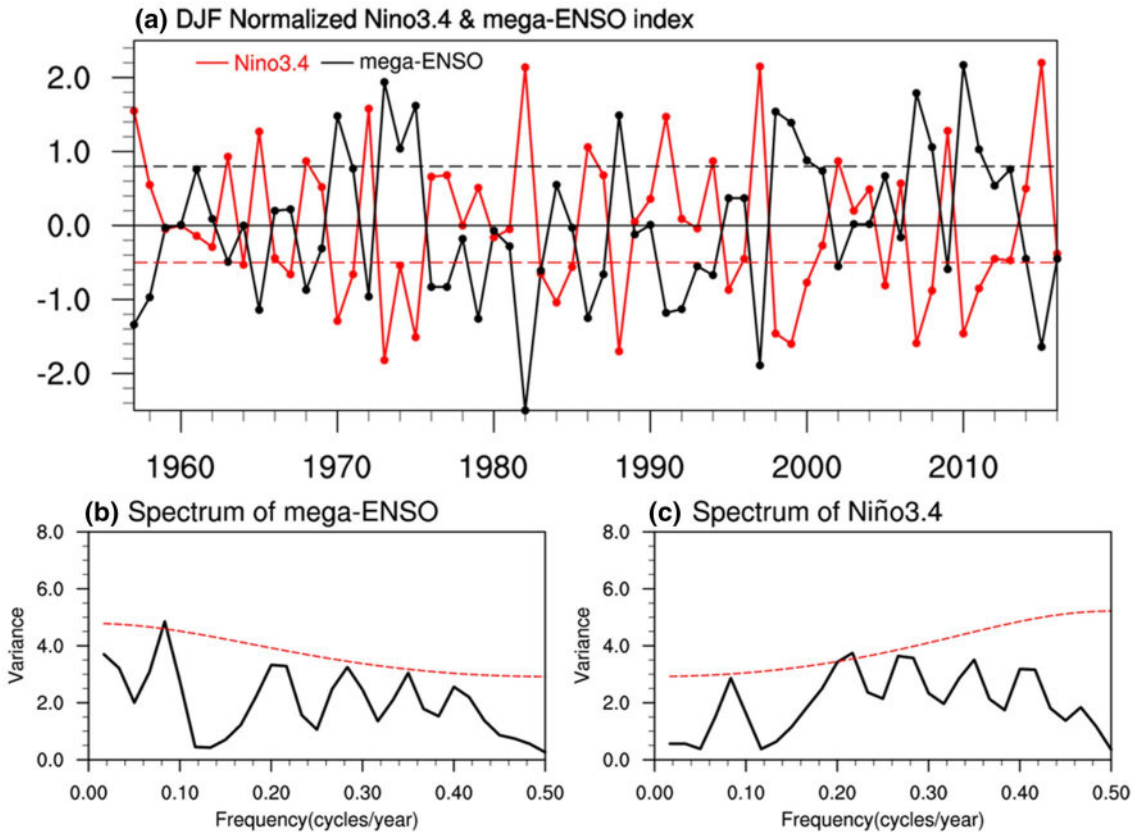

Fig. 2 **a** Time series of DJF Niño3.4 and mega-ENSO indices. Black (red) dash line denotes −0.5 (0.8). **b**, **c** Corresponding the power spectrum of the mega-ENSO and Nino3.4 indices

(Roeckner et al. 2003) is introduced to elucidate the potential mechanisms. As an AGCM that developed from the European Centre of Medium-Term Weather Forecast (ECMWF) model, ECHAM5.4 has been actively used for climate studies. In this study, the version used is triangular 63 horizontal resolutions with 19 vertical levels (T63L19). Based on this model, we conducted five experiments. First, we performed the control experiments, in which AMIP II historical SST was prescribed for twelve randomly selected sample years (all are ENSO-neutral years). For each sample, the simulation was integrated for 38 months and the last 3 months result was used as the reference. Such as 1958, the control run was integrated from 1 January 1956 to 28 February 1959. We took the results from 1 December 1958 to 28 February 1959 as samples. Then, four sensitivity experiments were performed, for which the observational SSTA was imposed on the wintertime (DJF) historical SSTs. The initial conditions obtained from the control run were used to integrate the sensitivity simulations from 1 December to 28 February for each sample. The details are displayed in Table 1.

3 Comparison of the different category of La Niña and related EAWM

Due to the high correlation between mega-ENSO (Wang et al. 2013) and Niño3.4 indices, conventional ENSO and mega-ENSO events may occur concurrently. The Niño3.4 and mega-ENSO indices are both introduced to better identify the mega-La Niña and Eq.La Niña winters. Using the criterion mentioned in Sect. 2, we selected twelve mega-La Niña winters (1970, 1973, 1974, 1975, 1988, 1998, 1999, 2000, 2007, 2008, 2010 and 2011) and eight Eq.La Niña winters (1964, 1967, 1971, 1983, 1984, 1985, 1995 and 2005) from 1957 to 2016.

Figure 3 displays the composite maps of DJF SSTAs in the Pacific and 2 m temperature (T2m) anomalies over

Table 1 List of SST perturbation experiments conducted in this study

Experiments	Description of SSt perturbation
Mega-La Niña	SSTA associated with mega-La Niña events is imposed in the Pacific (30°S–30°N, 120°E–100°W)
Weak mega-La Niña	SSTA associated with weak mega-La Niña events is imposed in the tropical Pacific (15°S–15°N, 120°E–100°W)
Eq.La Niña	SSTA associated with Eq.La Niña events is imposed in the tropical Pacific (15°S–15°N, 120°E–70°W)
Mega-EP La La Niña	K-shape positive SSTA associated with mega-La Niña and eastern Pacific negative SSTA associated with Eq.La Niña events (multiply by 1.8) are imposed in the Pacific (30°S–30°N, 120°E–70°W)

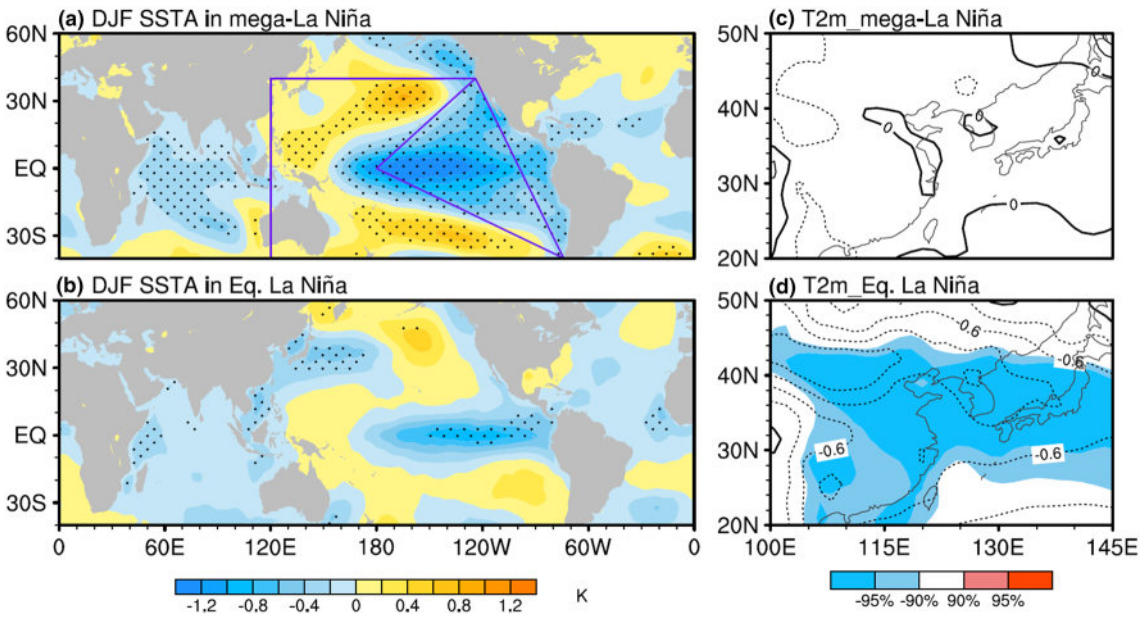

Fig. 3 DJF sea surface temperature (SST, K) anomalies of **a** mega-La Niña, **b** Eq.La Niña. **c, d** Are the same as (**a, b**), except for T2m (K). The black dots in each panel represent the region with anomalies significant at the 95% confidence level (Student's t test). The purple lines in **a** outlines the EP triangle and western Pacific K-shape regions where the mega-ENSO index is defined

the EA region for the two kinds of La Niña events. During mega-La Niña winters, an obvious positive K-shaped SSTA is detected in the western and subtropical Pacific with a negative triangle SSTA in the EP (Fig. 3a, purple box), which is in accordance with the defined mega-ENSO SSTA pattern (Wang et al. 2013). For Eq.La Niña cases, a significant narrow banded negative SSTA displays in the tropical EP (Fig. 3b). Interestingly, except for the ranges of the SSTA, the intensity and maximum center of tropical Pacific SSTA for the mega- and Eq.La Niña are also different. The relatively weak maximum cooling center of SSTA for the Eq.La Niña shifts eastward compared with its mega-La Niña counterpart. Furthermore, since the two kinds of La Niña have such diverse features, what are their impacts onto the EAWM? To answer this question, Fig. 3c, d give the large-scale spatial distribution of DJF T2m anomalies over EA (20°–50°N, 100°–145°E) for the mega- and Eq.La Niña. Corresponding to the mega-La Niña, there is no salient T2m anomaly over the EA region (Fig. 3c). In contrast, significant cooling T2m anomaly dominates East China, Korea, and Japan during the Eq.La Niña winter (Fig. 3d), which is consistent with the T2m southern mode.

Because of the distinct SSTA patterns, two types of La Niña-related tropical vertical convective motions are expected to be different. The omega fields at 500 hPa (omega-500) are checked. In the mega-La Niña cases, the positive omega-500 anomalies are centered over the tropical central Pacific, and the negative center covers the Maritime Continent (Fig. 4a). The anomalous descending (ascending) motion is also centered over the equatorial central Pacific (Maritime Continent) but shifts a bit eastward for the Eq.La Niña (Fig. 4b). Meanwhile, the intensity of omega-500 anomalies associated with the mega-La Niña SSTA is evidently larger than that of the Eq.La Niña. Although the vertical motions responded to the Eq.La Niña are weaker than that to the mega-La Niña, why does the EAWM show a stronger response? Next, we compared the atmospheric anomalies associated with the mega- and Eq.La Niña in the hope of answering this question.

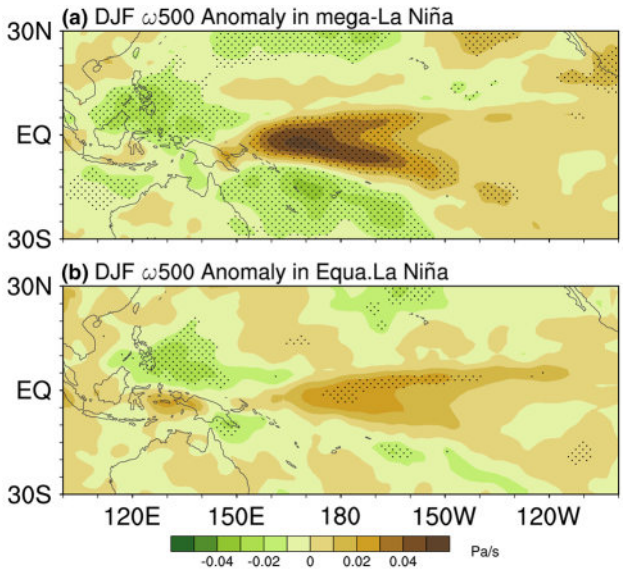

Fig. 4 DJF 500 hPa vertical velocity (omega-500, Pa/s) anomalies of **a** mega-La Niña, **b** Eq.La Niña. The black dots in each panel represent the region with anomalies significant at the 90% confidence level (Student's t test)

4 Contrasting dynamic structures of equatorial and mega-La Niña

4.1 Planetary-scale circulation anomalies associated with Eq. and mega-La Niña

The intensity and distribution of SSTA vary among individual ENSO events (Capotondi et al. 2015). The different flavors of ENSO may result in large discrepancies in the atmospheric and climatic responses over the extratropical regions (Horel and Wallace 1981; Lau and Nath 1996; Wang et al. 2000; Alexander et al. 2002). In this part, we mainly focus on the atmospheric anomalies related to the two kinds of La Niña.

Figure 5a, b displays the surface circulation anomalies associated with the mega- and Eq.La Niña. During mega-La Niña winter, a salient positive SLP anomaly occupies the northern Pacific. However, there are no salient SLP anomalies over the EA continent. Meanwhile, the Western North Pacific (WNP) cyclone is confined over the ocean area (Fig. 5a). This environment is unfavorable for the anomalous northerlies penetrating the EA continent, leading to a neutral EAWM. However, over the NP, the SLP anomalies for the Eq.La Niña markedly differs from that for the mega-La Niña. A huge SLP anomaly is located over the entire Eurasian continent, with one ridge elongating southward along the Caspian Sea to the Arabian Sea and another prominent ridge elongating southward from Mongolia toward the South China Sea (Fig. 5b). The latter reflects the intrusion of the cold-air along the "northwest pathway" from Mongolia all the way down to Southeast Asia. Meanwhile, an anomalous low centered over the subtropical NP (around 30°N, 190°W), generating a large zonal gradient between the subtropical ocean and continent. The strong gradient indicates heavy abnormal northerlies over EA from 55°N to the tropical region.

Figure 5c, d compare the large-scale horizontal wind and geopotential height anomalies at mid-troposphere (Z500, UV500) associated with the mega-La Niña and Eq.La Niña. For the mega-La Niña, the Z500 and UV500 anomaly patterns (Fig. 5c) are highly resemble that in the surface level (Fig. 5a). During the Eq.La Niña winters, a gigantic

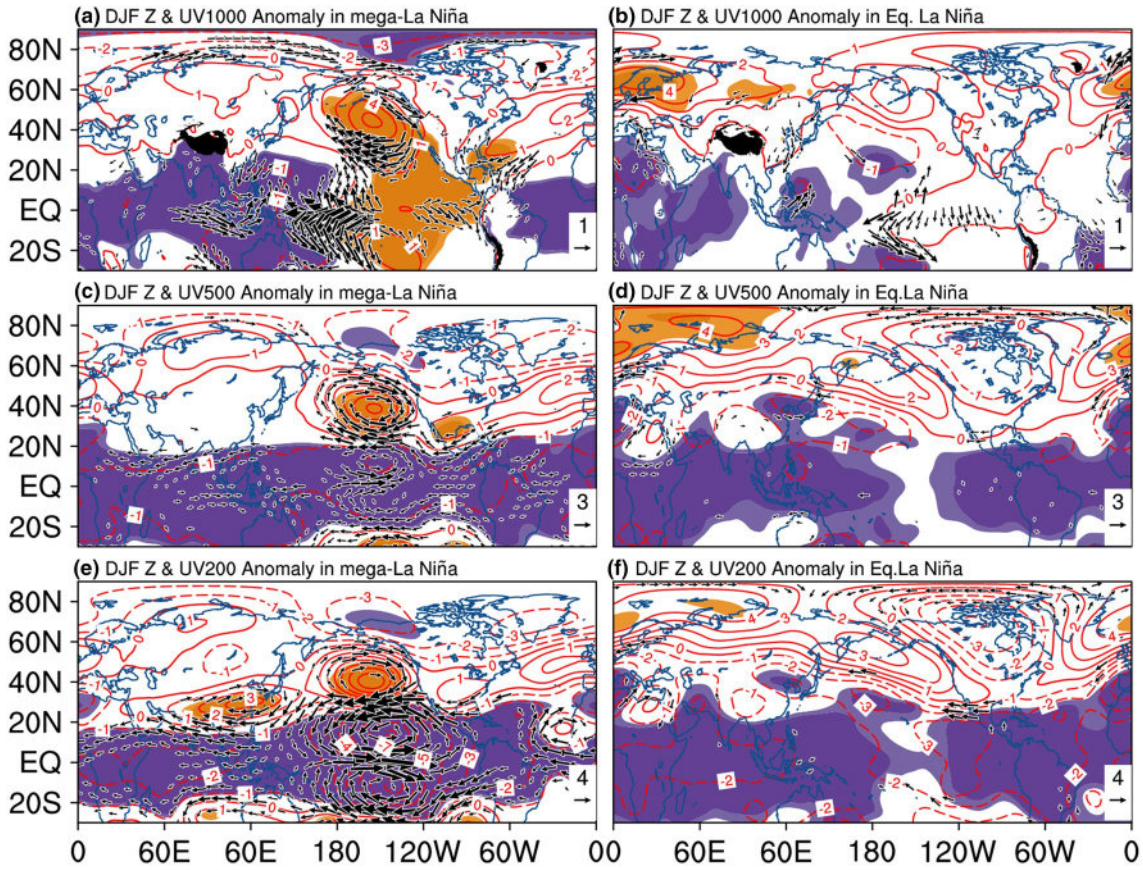

Fig. 5 DJF SLP (hPa) and UV10m (m/s) anomalies of **a** mega-La Niña, **b** Eq.La Niña. The vectors in each panel represent the region with anomalies significant at the 90% confidence level (Student's t test). The shaded areas exceeding the 90% and 95% confidence level based on the Student's t test. **c, d** Same as **a, b**, except for 500 hPa geopotential height (Z500, m) and winds (UV500) and **e, f** for 200 hPa geopotential height (Z200) and winds (UV200). The black shading in **a, b** represents the Tibetan Plateau

extended anticyclonic anomaly covers entire high-latitude Eurasia and North Pacific (Fig. 5d). A salient barotropic anomalous low is centered in the subtropical NP (around 35°N, 175°W) and extending westward to the Kearon Peninsula (around 40°N, 130°E)—indicating a reinforced and southward shifted East Asian trough (EAT) (compared with Wang et al. 2010b, Fig. 7a)—which may exert a great impact on the EAWM.

Figure 5e, f show the Z200 and UV200 anomalies related to the mega- and Eq.La Niña. Over the NP, an anticyclonic Z200 anomaly implies a weakened Aleutian Low, whereas no significant anomaly appears over the extratropical Eurasian during the mega-La Niña winter (Fig. 5e). For the Eq.La Niña (Fig. 5f), the anomalous Z200 patterns are similar to the mid-troposphere, with a significant banded negative anomaly centered over the subtropical North Pacific and the Kearon Peninsula, meanwhile, an anticyclonic anomaly covering high-latitude Eurasia and NP.

It needs to be pointed out that the strong WNP cyclone during the mega-La Niña winter may not exert a significant forcing on the EAWM (Fig. 5a). Zhang et al. (2015a) pointed out that during La Niña winter, intraseasonal signals dominate the atmospheric variations over WNP, resulting in a weak response of the circulation on the interannual timescale. This may be another reason for the weak connection of mega-La Niña and EAWM.

4.2 The impact of weak mega-La Niña

Considering the magnitude of mega-La Niña SSTAs are much larger than that of Eq.La Niña, it is hard to conclude that the different atmospheric anomalies response to the mega-La Niña and Eq.La Niña is depended on the SSTA intensity or the SSTA distribution pattern. In this part, 4 weak mega-La Niña years (1974, 2000, 2008, 2011) are selected to inspect the related SST anomaly and atmospheric response.

Figure 6 gives the composite maps of SST and circulation anomalies for the weak mega-La Niña. Salient warming SSTAs appears in the extratropical Pacific, with some cooling SSTA observed in the tropical central and eastern Pacific. This is similar to the defined areas of a mega-ENSO.

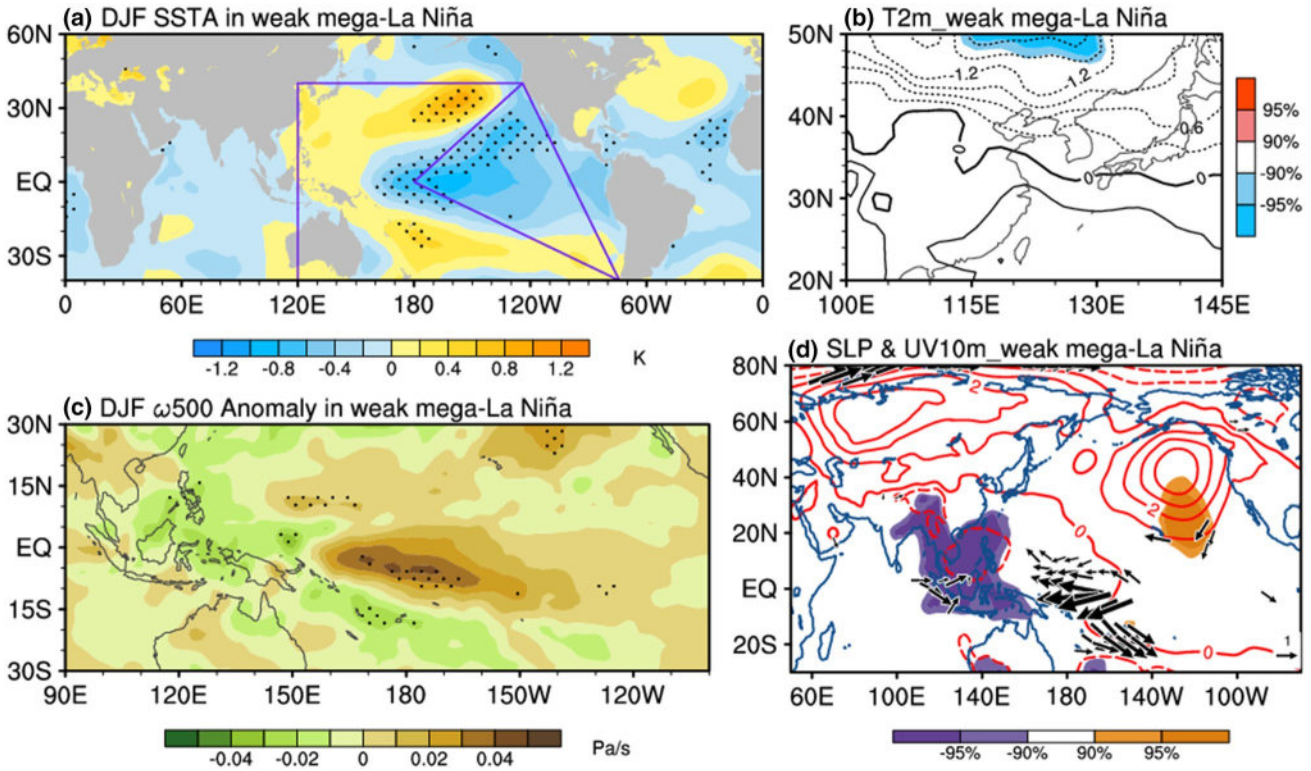

Fig. 6 Same as Figs. 3, 4, and 5, except for the weak mega-La Niña

Moreover, the SSTA maximum center of the weak mega-La Niña is also seated in the tropical central Pacific (Fig. 6a) and the resultant positive omega-500 anomaly is centered to the west of the data line (Fig. 6c). In response to this omega-500 anomaly, the atmospheric anomaly exhibits a salient anomalous high in SLP over NP and a neutral SLP anomaly over Eurasia (Fig. 6d). The underlying SST and upper layer circulation responses for the weak mega-La Niña present the spatial distributions in agreement with those of mega-La Niña. The T2m anomaly exhibits a mild EAWM over the subtropical regions of China, the Korean Peninsula and Japan (Fig. 6b).

5 Physical mechanisms

5.1 Why can't mega-ENSO enhance the EAWM?

Based on the comparison of three types of La Niña, we speculate that the changing SSTA distribution pattern may be the key reason for modulating the links of the tropical Pacific and EAWM. For the mega-La Niña, the cooling center of SSTA seated in the tropical central Pacific (Figs. 3a, 6a) with a convective descending motion centered to the west of the dateline (Figs. 4a, 6c), a poleward-propagating Rossby wave train respond to the central Pacific cooling is generated with its positive anomalous center located over NP, indicating a weakened Aleutian Low (Fig. 5c). The former studies of Lau and Nath (1990) and Alexander et al. (2004) have pointed out that the atmosphere is likely to trigger the ENSO-related extratropical Pacific SSTAs, not vice versa. Such as during the mega-La Niña winter, the NP SSTAs show an apparently wind driven pattern: the central Pacific cooling SSTA induces a gigantic anticyclone covering from the tropical to extratropical NP. Anomalous northeasterly flow along the eastern flank of the anomalous NP high weakens westerlies in the subtropical NP and speed up the trades over the Eastern North Pacific (ENP) (Figs. 4a, 6c). The resulting wind speed—weaker in the subtropics and stronger in the ENP—induces SSTA changes in the NP basin: the structure resembles the pattern of mega-ENSO. Meanwhile, the huge anticyclone reduces the zonal gradient between NP and EA continent, unfavorable for the enhancement of EAWM. The weak mega-La Niña shows similar characteristics (Fig. 6).

However, the composites do not guarantee any cause and effect. To confirm whether the different types of La Niña can trigger the disparate atmospheric responses or the opposite way around. We perform a series of experiments using the ECHAM (v5.4) model. Firstly, the SSTA associated with mega-La Niña in the Pacific Ocean (Figs. 3a, 6a) are imposed in the wintertime (DJF) SST field. It should point out that we imposed a broader SSTA on the region

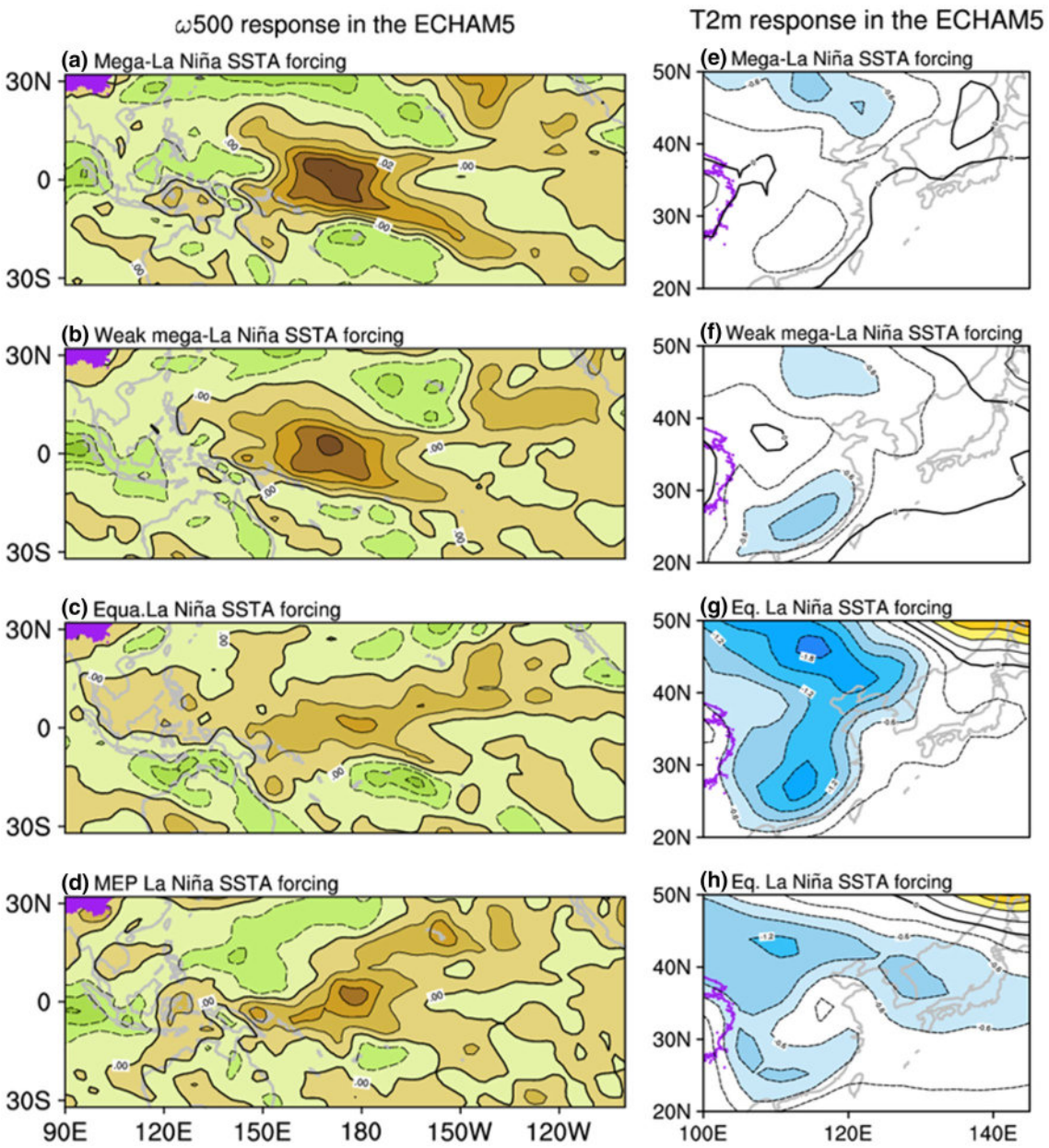

Fig. 7 **a** Tropical omega-500 responses in the ECHAM5 regarding a difference between mega-La Niña forcing and control run. **b**–**d** Same as **a** but for weak mega-La Niña, Eq.La Niña and MEP La Niña forcing. **e**–**h** Are the corresponding T2m anomalies. The shaded areas in **e**–**h** indicate anomalous values above 0.6 K or below − 0.6 K. Contour interval is 0.6 K

of 30°S–30°N, 120°E–100°W in the mega-La Niña simulation to mimic the contribution of entire mega-ENSO type of SSTA. For the weak mega-La Niña experiment, the SSTA is added to the tropical region (15°S–15°N, 120°E–100°W) for the reasons: (1) it contains nearly the same area as well as the same intensity to the Eq.La Niña forcing, providing a more intuitive way to compare the impact of the shift of the SSTA maximum center in the same level; (2) making sure whether the equatorial central Pacific cooling can trigger an NP anticyclone response directly. By checking the differences of sensitivity and control runs, the simulated omega-500 patterns show high similarity with the observation (Figs. 4a, 6c), with anomalous descending motion situated to the west of the dateline in response to the strong and weak mega-La Niña forcing (Fig. 7a, b). The corresponding simulated T2m anomalies (Fig. 7e, f) are also similar to the observed ones (Figs. 3c, 6b). The resultant T2m anomalies show a relatively mild winter thought out the subtropical EA region. Further analysis of the related circulation filed revealed that mega-La Niña-type or the central Pacific

cooling SSTA forcing excites an anomalous high over NP (Fig. 8a, b) that reduces the zonal gradient between anomalous NP high and SLP anomalies over EA continent, implying the weak northerlies and a mild EAWM. The results are in accordance with the observations.

5.2 How does Eq.La Niña affect EAWM

The aforementioned analysis has explained the reasons for the uncoupling relationship of the mega-ENSO and EAWM. But, how does the Eq.La Niña influence the EAWM? The simulated results further confirmed that when the SSTA is added to the tropical Pacific (15°S–15°N, 120°E–70°W) with the cooling SSTA centered in the equatorial EP, the resulting convective descending motion shifts eastward (Fig. 7c) compared to the mega-La Niña forcing (Fig. 7a, b). An anomalous low in the SLP over the subtropical NP is triggered with the abnormal northerlies in its west flank that coming down from 50°N to South China. Meanwhile, an anomalous high over the North of EA and NP is observed with an obvious SLP ridge extending southward from Mongolia to South China (Fig. 8c). In the mid-troposphere,

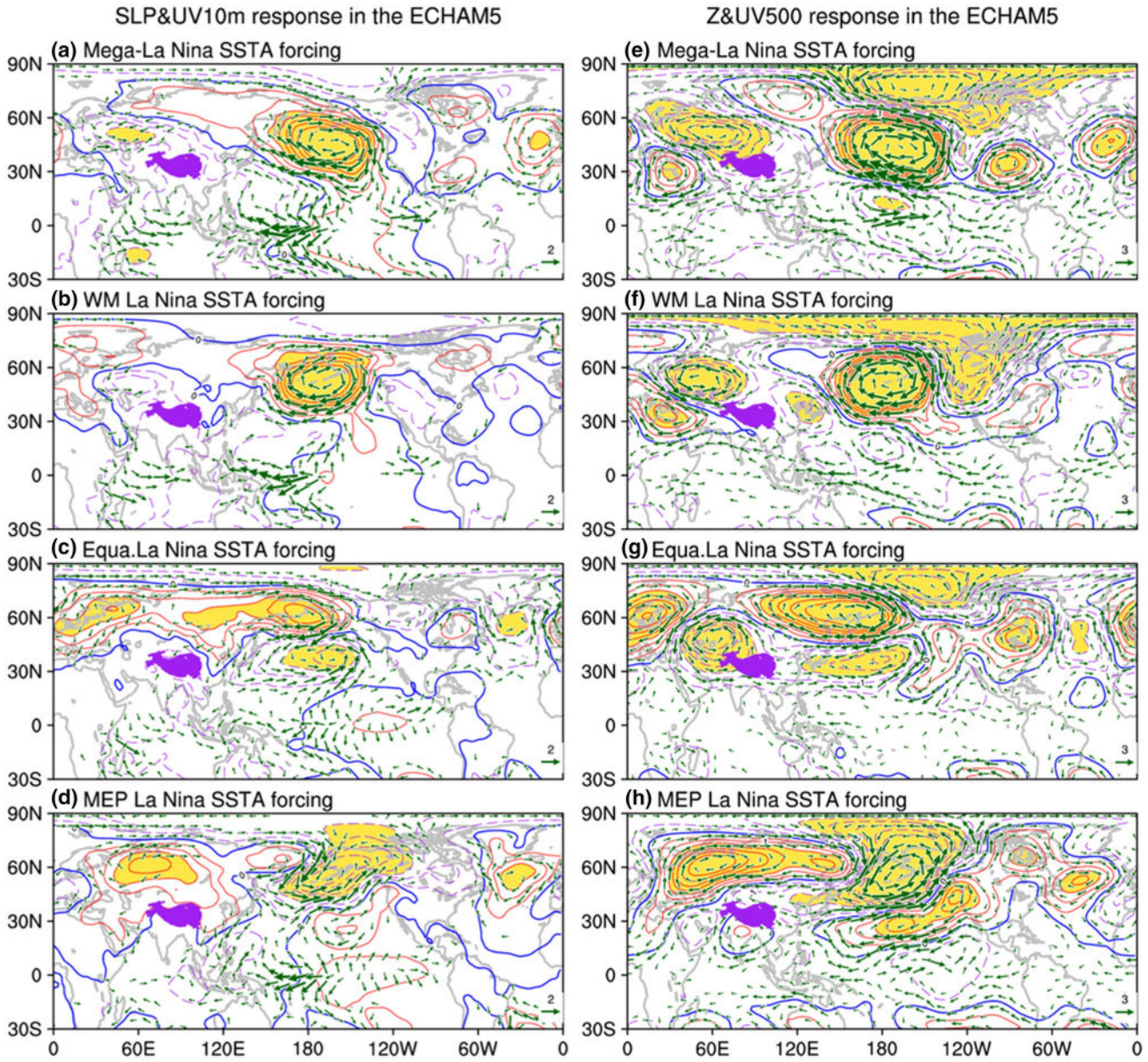

Fig. 8 The SLP (hPa) and UV10m (m/s) (**a**–**d**), Z and UV500 (**b**–**f**). The shaded areas indicate SLP values above 1.5 hPa or below − 1.5 hPa. Contour interval is 0.5 hPa. The vectors indicate wind speed above 0.6 m/s or below − 0.6 m/s. The purple shading represents the Tibetan Plateau

Z500 basically responds a deepened and southward shifted East Asian trough over EA and reinforced anomalous high over northern Eurasia, which is similar to the observation (Fig. 5d). In addition, an atmospheric teleconnection pattern from subtropical NP, though extra-tropical NP and North America, to northern Eurasia (Fig. 8f), can also be found, which may connect tropic forcing and the high pressure over northern Eurasia. All these circumstances favor the reinforcement of the EAWM (Fig. 7g). However, the anomalies high over extratropical NP and the anomalous low over North America shifted a bit westward compared with the observation (Fig. 5d).

Here, based on the observational and simulated results, the process through which Eq.La Niña impacts EAWM is concluded as follows: In the tropical Pacific, maximum SSTA is centered over the EP that excites a convective descending motion located to the east of the dateline (Figs. 4b, 7c). Differing from the tropical central Pacific cooling that generates a huge anticyclonic anomaly residing over NP (Figs. 5a, 8a). On the one hand, at the surface level, EP cooling excites an anomalous barotropic low in the subtropical NP and a gigantic anomalous high over northern Eurasia (Figs. 5b, 8c). The strong zonal gradient between anomalous NP low and EA continent high favor the penetration of the northerly anomalies from north to south. On the other hand, the anomalous low extends westward to the Korean Peninsula at the middle and upper troposphere—indicating a deeper and southward shifted EAT, exerting a notable forcing on the EAWM (Figs. 5d, 8f). The surface and mid-high level circulation anomalies work together to enhance the EAWM.

6 Conclusion and discussion

6.1 Conclusion

In this study, using observational data and numerical simulation, the impacts of La Niña on T2m over EA in winter are investigated. Two types of events are identified—the mega-La Niña and the Eq.La Niña. Mega-La Niña shows a western and subtropical Pacific K-shape warming SSTA and a tropical central Pacific triangle cooling SSTA. The corresponding T2m anomaly over EA exhibits a neutral condition. Nevertheless, during the Eq.La Niña winter, the maximum SSTA center shifts eastward with a notable cooling SSTA centered mainly in the tropical EP and its magnitude is much weaker than its mega-La Niña counterpart. However, the associated T2m anomaly shows a significant cooling throughout East China, the Korean Peninsula and Japan, implying a strong EAWM. Such T2m anomaly pattern is similar to the distribution of surface temperature southern mode, which is defined by Wang et al. (2010b).

The related physical mechanism reveals that during the mega-La Niña winter, tropical central Pacific cooling generates a convective descending motion to the west of the dateline. A poleward-propagating Rossby wave is triggered with a significant anomalous high over NP—indicating a weakened Aleutian Low—and a neutral SLP anomaly over the north of Eurasia. On the one hand, northeasterly flow along the eastern flank of the anomalous NP high weakens the westerlies in the subtropical NP and speed up the trades over the ENP, inducing the SSTA pattern in the subtropical basin that resembles mega-ENSO. On the other hand, the weak zonal gradient between anomalous NP high and EA continent low does not favor the enhancement of the northerlies over EA, resulting in a weak EAWM. For the Eq.La Niña, on the surface level, the equatorial EP cooling generates an anomalous low over the subtropical NP and a gigantic anomalous continental high over northern Eurasia. The strong zonal gradient between them indicates the enhanced anomalous northerlies over EA from the north down to the south. Over the middle and upper-level troposphere, a strengthened and southward shifted EAT exert a great forcing on the EAWM. Both processes are working together that could induce a significantly strong EAWM.

It is interesting to notice that almost all mega-La Niña can also be recognized as the central Pacific (CP) La Niña events for the maximum SSTA centering the tropical central Pacific. For the Eq.La Niña, the maximum SSTA is situated in the tropical EP, which can be seen as the EP (EP) La Niña events. It had been assumed that La Niña events could not be divided according to the locations of the maximum SSTA centers. For example, based on the observational and model results, Kug and Ham (2011) pointed out that the conventional La Niña and La Niña Modoki-related SST and precipitation patterns were hard to be distinguished. Recently, by analyzing the spatial patterns of SSTA, Zhang et al. (2015b) successfully classified La Niña into CP and EP events over the period of 1951–2009 to study their different impacts on the climate of northern Europe. However, their method primarily relies on subjective judgments. Our method, however, provides an objective criterion. The specific years selected from 1957 to 2009 by the subjective judgments (Zhang et al. 2015b) and our objective criteria are listed in Table 2. In order to contrast two methods, we also checked the SSTA patterns for each year (Fig. 9). Although during 1970, 1999, and 2007 winter, the La Niña events are selected as the mixed type by the subjective judgment (Zhang et al. 2015b), they are referred to as the mega-La Niña years according to our objective criteria due to the salient K-shape warming SSTA (the composite with or without the variables in this year does not influence qualitative results). Besides, 2008 is a mega-La Niña (CP) year, 1967 and 1985 are the Eq.La Niña (EP) years. The 3 years are not given by Zhang et al.

Table 2 La Niña event classification using the subjective and objective methods

	Events	Years
Objective method	Mega-La Niña	1970, 1973, 1974, 1975, 1988, 1998, 1999, 2000, 2007, 2008, 2010, 2011 (12)
	Eq.La Niña	1964, 1967, 1971, 1983, 1984, 1985, 1995, 2005 (8)
Subjective method	CP La Niña	1973, 1974, 1975, 1983, 1988, 1998, 2000 (7)
	EP La Niña	1964, 1971, 1984, 1995, 2005 (4)
	Mixed La Niña	1970, 1999, 2007 (3)

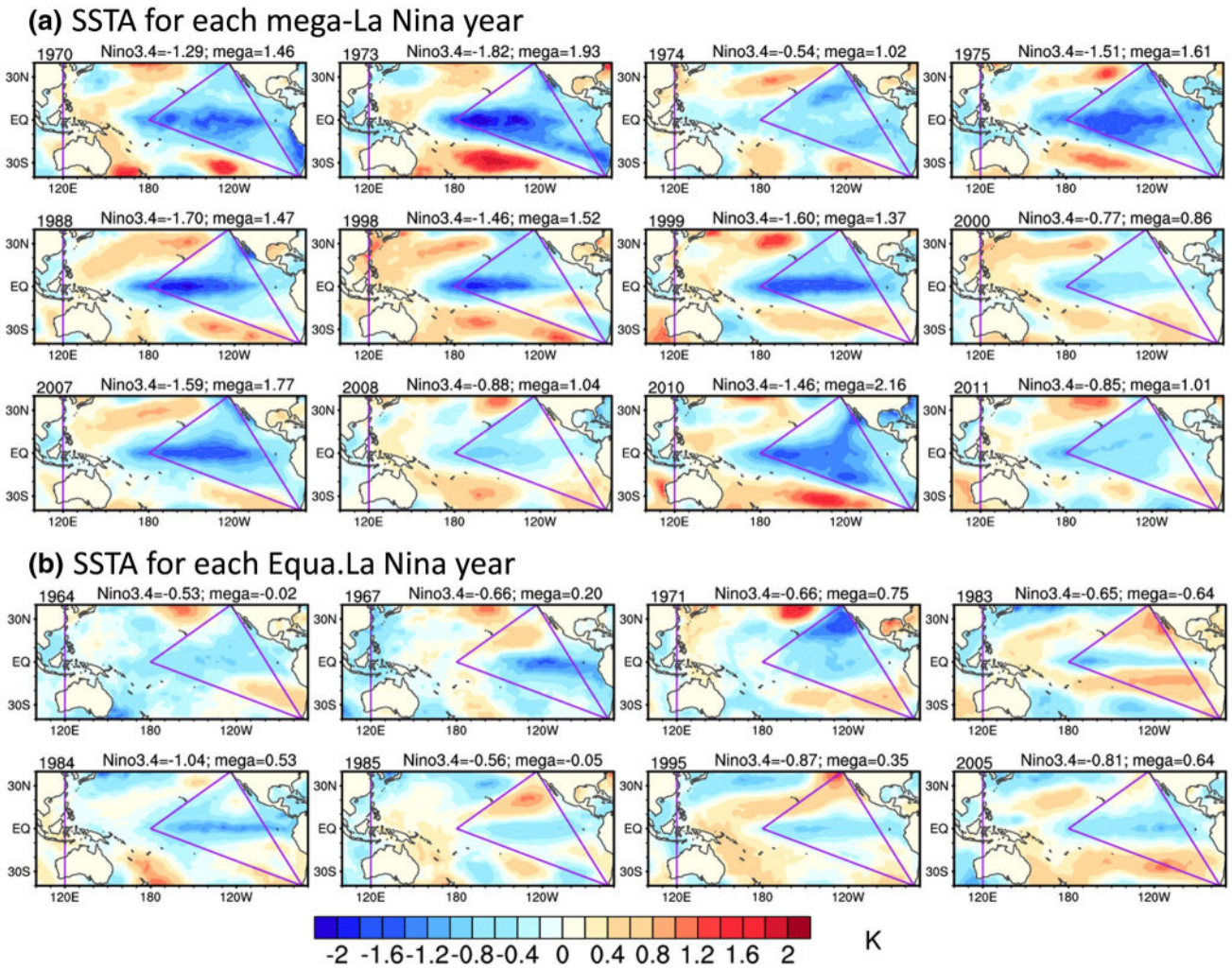

Fig. 9 The SSTAs (K) for each **a** mega-La Niña, **b** Eq.La Niña events. The purple lines outline the EP triangle and western Pacific K-shape regions where the mega-ENSO index is defined. Shading intervals are 0.2 K

(2015b). The only exception is 1983, the maximum SSTA centered in the tropical CP. As a CP La Niña, it is grouped into the Eq.La Niña by using our criteria. The reason may be the SSTA in the triangle region shows a tripolar mode rather than the mono-sign cooling, resulting in a small mega-ENSO index value. However, 19 out of 20 La Niña events are rightly classified. Our criteria provide a convenient and objective way for which La Niña events can be divided according to the range as well as the location of the SSTA maximum center.

In contrast to La Niña events, when the El Niño events are classified using our criteria into mega-El Niño and Eq.El Niño, CP and EP El Niños seem to be mere random chances among the two types of El Niño. And the two types of El Niño are not significantly impacting the surface temperature southern mode. In other words, this phenomenon reflects

an asymmetric atmospheric response to the warm and cold ENSO events, which might be explained by the asymmetric SSTA patterns and the associated air-sea coupling systems (Hoerling et al. 1997; Feng and Li 2011).

To sum up, the different La Niña would exert different impacts on EAWM. Although Eq.La Niña exhibits a narrower spatial pattern and a weaker SSTA intensity, it shows a more intimate relationship with EAWM than its mega-La Niña counterpart. The climatic impacts of the Eq.La Niña, therefore, cannot be neglected. However, through what mechanism does Eq.La Niña be triggered? And, whether the mega-La Niña and Eq.La Niña events can also be detected during other seasons? These questions need further investigation.

6.2 Discussion

From the observational results, the Eq.La Niña (mega-La Niña) mostly corresponding to the tropical EP (CP) cooling and weak (strong) east–west Pacific gradient. What will happy if a mega-La Niña event corresponding to the tropical EP cooling? We performed another sensitivity experiment, named mega-EP La Niña (MEP_LN), to answer this question. In the MEP_LN experiment, the SSTA is added on the region of 30°S–30°N, 120°E–90°W. The imposed western Pacific positive K-shape (negative tropical east Pacific) SSTA is obtained from mega-La Niña (Eq.La Niña) forcing. Considering the tropical east Pacific negative SSTA for Eq.La Niña forcing is much smaller than that of mega-La Niña forcing. The negative SSTA is multiplied by 1.8 to guarantee a similar intensity. Therefore, compared with the mega-La Niña experiment, the zonal location of positive SSTA shifted eastward for the MEP_LN forcing. Compared with the Eq.La Niña experiment, the MEP_LN forcing processed a much larger east–west gradient.

Under the MEP_LN forcing, SLP responds an anomalous low over NP and a reinforced anomalous high over northern Eurasia (Fig. 8d). In the mid-troposphere, a deepened East Asian trough appears over the EA (Fig. 8h). The surface and mid-troposphere anomalous low, however, seems northward shifted in contrast with the Eq.La Nina forcing (Fig. 8c, f). In addition, although the imposed eastern Pacific negative SSTA is much stronger than Eq.La Nina forcing, the intensity of T2m anomalies over southern EA are weaker than that of Eq.La Nina forcing (Fig. 7g, h). The reasons may due to the impact of the convective activities around Kalimantan Island. When the western Pacific positive SSTAs are imposed (removed), omega-500 basically response the negative (positive) anomalies around Kalimantan Island (Fig. 7a–d), indicating the ascending (descending) movements, which are in accordance with the observations (Fig. 4).

The numerical results meant that the zonal location of anomalous SST/descent on the tropical central/eastern Pacific is important to explain the different atmospheric responses during the strong gradient La Niña years. However, the strong western Pacific warming SSTA may reduce the impacts of tropical eastern Pacific cooling SSTA on the cold EAWM T2m southern mode. At last, it needs more observational evidence to verify the numerical results.

Acknowledgements This work is jointly supported by the National Natural Science Foundation of China (NSFC) (Grant No. 41790475), the National Key Research & Development Program of China (Grant No. 2016YFA0601801), the Ministry of Science and Technology of China (Grant Nos. 2015CB953904 and 2015CB453201) and the NSFC (Grant Nos. 91637312, 41575075 and 91437216).

References

Alexander MA, Bladé I, Newman M, Lanzante JR, Lau NC, Scott JD (2002) The atmospheric bridge: The influence of ENSO teleconnections on air–sea interaction over the global oceans. J Clim 15:2205–2231

Alexander MA, Lau NC, Scott JD (2004) Broadening the atmospheric bridge paradigm: ENSO teleconnections to the tropical West Pacific–Indian Oceans over the seasonal cycle and to the North Pacific in summer. In: Wang C, Xie SP, Carton J (eds) Earth's climate: the ocean–atmosphere interaction. AGU monograph, vol 147. American Geophysical Union, Washington, DC, pp 85–104. https://doi.org/10.1029/147GM05

Capotondi A, Wittenberg AT, Newman M, Di Lorenzo E, Yu JY et al (2015) Understanding ENSO diversity. Bull Am Meteorol Soc 96(6):921–938

Chen W (2002) Impacts of El Niño and La Niña on the cycle of the East Asian winter and summer monsoon. Chin J Atmos Sci 26:595–610 (**in Chinese**)

Chen W, Graf HF, Huang RH (2000) The interannual variability of East Asian winter monsoon and its relation to the summer monsoon. Adv Atmos Sci 17:48–60

Chen Z, Wu R, Chen W (2014) Distinguishing interannual variations of the northern and southern modes of the East Asian winter monsoon. J Clim 27:835–851

Dee DP, Uppala SM, Simmons AJ, Berrisford P, Poli P, Kobayashi S, Andrae U, Balmaseda MA, Balsamo G, Bauer P, Bechtold P (2011) The ERA-Interim reanalysis: Configuration and performance of the data assimilation system. Q J R Meteor Soc 137:553–597

Feng J, Li JP (2011) Influence of El Niño Modoki on spring rainfall over south China. J Geophys Res Atmos 116:D13102. https://doi.org/10.1029/2010JD015160

Gong DY, Wang SW, Zhu JH (2001) East Asian winter monsoon and Arctic oscillation. Geophys Res Lett 28:2073–2076

Ha KJ, Heo KY, Lee SS, Yun KS, Jhun JG (2012) Variability in the East Asian monsoon: a review. Meteo Appl 19:200–215

Hamed KH, Rao AR (1998) A modified Mann-Kendall trend test for autocorrelated data. J Hydrometeor 204:182–196

He SP, Wang HJ (2013) Oscillating Relationship between the East Asian Winter Monsoon and ENSO. J Clim 26:9819–9838

Hoerling MP, Kumar A, Zhong M (1997) El Niño, La Niña, and the nonlinearity of their teleconnections. J Clim 10:1769–1786

Horel JD, Wallace JM (1981) Planetary-scale atmospheric phenomena associated with the Southern Oscillation. Mon Weather Rev 109:813–829

Huang B, Banzon VF, Freeman E, Lawrimore J, Liu W, Peterson TC, Smith TM, Thorne PW, Woodruff SD, Zhang HM (2014) Extended reconstructed sea surface temperature version 4 (ERSST.v4): Part I. upgrades and intercomparisons. J Clim 28:911–930

Huang B, Thorne P, Smith T, Liu W, Lawrimore J, Banzon V, Zhang H, Peterson T, Menne M (2015) Further exploring and quantifying uncertainties for extended reconstructed sea surface temperature (ERSST) Version 4 (v4). J Clim 29:3119–3142. https://doi.org/10.1175/JCLI-D-15-0430.1

Jhun JG, Lee EJ (2004) A new East Asian winter monsoon index and associated characteristics of winter monsoon. J Clim 17:711–726

Jia X, Lin H, Ge J (2016) The interdecadal change of ENSO impact on wintertime East Asian climate. J Geophys Res 120:11918–11935. https://doi.org/10.1002/2015JD023583

Kug JS, Ham YG (2011) Are there two types of La Nina? Geophys Res Lett 38:L16704. https://doi.org/10.1029/2011GL048237

Lau NC, Nath MJ (1990) A general circulation model study of the atmospheric response to extratropical SST anomalies observed in 1950–79. J Clim 3:965–989

Lau NC, Nath MJ (1996) The role of the "atmospheric bridge" in linking tropical Pacific ENSO events to extratropical SST anomalies. J Clim 9:2036–2057

Liu W, Huang B, Thorne PW, Banzon VF, Zhang HM, Freeman E, Lawrimore J, Peterson TC, Smith TM, Woodruff SD (2014a) Extended Reconstructed Sea Surface Temperature version 4 (ERSST.v4): Part II. Parametric and structural uncertainty estimations. J Clim 28:931–951. https://doi.org/10.1175/JCLI-D-14-00007.1

Liu Y, Wang L, Zhou W, Chen W (2014b) Three Eurasian teleconnection patterns: spatial structures, temporal variability, and associated winter climate anomalies. Clim Dyns 42:2817–2839

Luo D, Xiao Y, Yao Y et al (2016) Impact of Ural blocking on winter Warm Arctic—cold Eurasian anomalies. Part II: the link to the North Atlantic Oscillation. J Clim 29:3949–3971

Mondal A, Kundu S, Mukhopadhyay A (2012) Rainfall trend analysis by Mann-Kendall test: a case study of north-eastern part of Cuttack district, Orissa. Int J Geol Earth Environ Sci 2:70–78

Parker D, Folland C, Scaife A, Knight J, Colman A, Baines P (2007) Decadal to multidecadal variability and the climate change background. J Geophys Res 112:1148–1154

Power S, Casey T, Folland C, Colman A, Mehta V (1999) Interdecadal modulation of the impact of ENSO on Australia. Clim Dyn 15:319–324

Rayner NA, Parkler DE, Horton EB, Folland CK, Alexander LV, Rowell DP, Kent EC, Kaplan A (2003) Global analyses of sea surface temperature, sea ice, and night marine air temperatures since the late nineteenth century. J Geophys Res 108(D14):4407. https://doi.org/10.1029/2002JD002670

Roeckner E, Bäuml G, Bonaventura L, Brokopf R, Esch M, Giorgetta M, Hagemann S, Kirchner I, Kornblueh L, Manzini E, Rhodin A, Schlese U, Schulzweida U, Tompkins A (2003) The atmospheric general circulation model ECHAM5: Part I: Model description. Max Planck Institute Rep. Report No. 349

Tao S, Zhang Q (1998) Response of the Asian winter and summer monsoon to ENSO events. Sci Atmos Sin 22:399–407 (**in Chinese**)

Tomita T, Yasunari T (1996) Role of the northeast winter monsoon on the biennial oscillation of the ENSO/monsoon system. J Meteor Soc Japan 74:399–413

Uppala SM, Kållberg PW, Simmons AJ, Andrae U, Bechtold VD, Fiorino M, Gibson JK, Haseler J, Hernandez A, Kelly GA, Li X (2005) The ERA-40 reanalysis. Q J R Meteor Soc 131:2961–3012

Wang HJ, He SP (2012) Weakening relationship between East Asian winter Monsoon and ENSO after mid-1970s. Chin Sci Bull 57:3535–3540

Wang L, Lu M (2017) The East Asian winter monsoon. In: Chang C-P (ed) The Global monsoon system: research and forecast, 3rd edn. World Scientific, Singapore, pp 51–61, https://doi.org/10.1142/9789813200913_0005

Wang B, Zhang Q (2002) Pacific–East Asian teleconnection. Part II: how the Philippine Sea anomalous anticyclone is established during El Niño development. J Clim 15:3252–3265

Wang B, Wu R, Fu X (2000) Pacific–East Asia teleconnection: how does ENSO affect East Asian climate? J Clim 13:1517–1536

Wang L, Chen W, Huang R (2008) Interdecadal modulation of PDO on the impact of ENSO on the East Asian winter monsoon. Geophys Res Lett 35:L20702. https://doi.org/10.1029/2008GL035287

Wang L, Chen W, Zhou W, Chan JC, Barriopedro D, Huang R (2010a) Effect of the climate shift around mid-1970 s on the relationship between wintertime ural blocking circulation and East Asian climate. Int J Climatol 30:153–158

Wang B, Wu Z, Chang C-P, Liu J, Li J, Zhou T (2010b) Another Look at interannual-to-interdecadal variations of the East Asian Winter Monsoon: the Northern and Southern temperature modes. J Clim 23:1495–1512

Wang B, Liu J, Kim HJ, Webster PJ, Yim SY, Xiang BQ (2013) Northern Hemisphere summer monsoon intensified by mega-El Niño/southern oscillation and Atlantic multidecadal oscillation. Proc Natl Acad Sci USA 14:5347–5352

Wang L, Liu Y, Zhang Y, Chen W, Chen S (2018) Time-varying structure of the wintertime Eurasian pattern: role of the North Atlantic sea surface temperature and atmospheric mean flow, Clim Dyns. https://doi.org/10.1007/s00382-018-4261-9

Wu B-Y, Huang RH (1999) Effects of the extremes in the North Atlantic oscillation on East Asia winter monsoon. Chin J Atmos Sci 23:641–651

Wu B-Y, Wang J (2002) Winter Arctic Oscillation, Siberian High and East Asian winter monsoon. Geophys Res Lett 29:1897. https://doi.org/10.1029/2002GL015373

Wu Z, Zhang P (2015) Interdecadal variability of the mega-ENSO–NAO synchronization in winter. Clim Dyn 45:1117–1128

Wu Z, Li J, Wang B, Liu X (2009) Can the Southern Hemisphere annular mode affect Chinese winter monsoon? J Geophys Res 114:D11107. https://doi.org/10.1029/2008JD011501

Zhang R, Sumi A, Kimoto M (1996) Impact of El Niño on the East Asian monsoon: a diagnostic study of the'86/87 and'91/92 events. J Meteor Soc Jpn 74:49–62

Zhang Y, Wallace JM, Battisti DS (1997) ENSO-like interdecadal variability. J Clim 10:1004–1020

Zhang R, Li T, Wen M, Liu L (2015a) Role of intraseasonal oscillation in asymmetric impacts of El Niño and La Niña on the rainfall over southern China in boreal winter. Clim Dyn 45:559–567

Zhang WJ, Wang L, Xiang BQ, Qi L, He JH (2015b) Impacts of two types of La Niña on the NAO during boreal winter. Clim Dyn 44:1351–1366. https://doi.org/10.1007/s00382-014-2155-z

Zhang L, Wu Z, Zhou Y (2016) Different impacts of typical and atypical enso on the indian summer rainfall: ENSO-developing phase. Atmos Ocean 54:440–456

Zhang P, Wu ZW, Chen H (2017) Interdecadal variability of the ENSO–North Pacific atmospheric circulation in winter. Atmos Ocean 55(2):110–120